International Journal of Fluid Mechanics & Thermal Sciences
2023; 9(1): 12-19
http://www.sciencepublishinggroup.com/j/ijfmts
doi: 10.11648/j.ijfmts.20230901.12
ISSN: 2469-8105 (Print); ISSN: 2469-8113 (Online)

Analysis of Water, Ethylene and Propylene Glycol-Based Nanofluids for Optimal Radiator Coolant

Hilder Mary Kisengese, Winifred Nduku Mutuku, Kimulu Ancent Makau

Department of Mathematics and Actuarial Science, Kenyatta University, Nairobi, Kenya

Email address:

kisehilder@gmail.com (Hilder Mary Kisengese), mutukuwinnie@gmail.com (Winifred Nduku Mutuku), ancentk@gmail.com (Kimulu Ancent Makau)

To cite this article:

Hilder Mary Kisengese, Winifred Nduku Mutuku, Kimulu Ancent Makau. Analysis of Water, Ethylene and Propylene Glycol-Based Nanofluids for Optimal Radiator Coolant. *International Journal of Fluid Mechanics & Thermal Sciences*. Vol. 9, No. 1, 2023, pp. 12-19. doi: 10.11648/j.ijfmts.20230901.12

Received: September 26, 2023; **Accepted**: October 14, 2023; **Published**: November 9, 2023

Abstract: Convection is the spontaneous movement of fluid phases, either single or multiple, driven by interactions with heterogeneous material properties and body forces such as density and gravity. This movement of heated fluid facilitates heat transfer within a system. Natural convection finds applications in heat dissipation, air conditioning, and microelectronics. However, industrial fluids commonly used for heat transfer, such as minerals, oil, water, and ethylene glycol (EG), face limitations due to their low thermal conductivities, hindering heat exchange efficiency. The production of efficient cost-effective cooling systems for automotive engines is a significant challenge in the automobile industry. Most engines depend on fluid for cooling and therefore use liquid coolants such as ethylene glycol and water, but with poor heat transmission properties. Nanoparticles, which have been shown to improve thermal conductivity, enhance the thermal properties of the fluids. This study compares six different radiator coolants; water-CuO, Propylene-glycol-CuO, ethylene-glycol-CuO, water-MgO, Propylene-glycol-MgO, and ethylene-glycol-MgO. Nanoparticles exhibit improved thermophysical qualities and therefore nanofluids are used as coolants in various mechanical and engineering contexts, including, but not limited to electronics, vehicles, transformers, computers, and electrical devices. The similarity transformation is utilized to non-dimensionalise the governing equations. The resulting equations are solved using a numerical method with the Runge-Kutta fourth-order method. The results show that water-based nanofluids provide the best coolant. However, when the radiator is close to the magnetic field emerging from the automobile engines, copper oxide or Magnesium oxide nanoparticles should be used with water as base fluid.

Keywords: Nanofluid, Nanoparticles, Base Fluid, Propylene Glycol, Ethylene Glycol

1. Introduction

Convection is the spontaneous movement of fluid phases, either single or multiple, driven by interactions with heterogeneous material properties and body forces such as density and gravity. This movement of heated fluid, such as air or water, facilitates heat transfer within a system. However, industrial fluids commonly used for heat transfer, such as minerals, oil, water and ethylene glycol, face limitations due to their low thermal conductivities which hinder heat exchange efficiency. As a result, nanofluids were invented, by dispersing nanometer-sized solid particles in a base fluid [1]. The base fluids used with the nanoparticles can be any of the conductive fluids like water, oil, polymer solutions, bio-fluids, or everyday fluids like paraffin. Nanofluids exhibit superior thermal physical properties, including higher thermal conductivity, thermal diffusivity, viscosity, and convective heat transfer coefficients [2-5]. The use of nanofluids in heat exchangers was studied by [6-8], who discovered a substantial opportunity for application in cooling and associated technologies. Ethylene glycol/copper nanofluids were studied by Murshed *et al.* [9], who found that their heat transfer rate was improved. It is demonstrated that ethylene glycol-based nanofluids have dramatically improved thermal physical characteristics when copper *Cu*, copper oxide *CuO*, aluminium oxide Al_2O_3, and titanium oxide TiO_2 nanoparticles are dispersed in the fluid. Kimulu et al. [10] used copper oxide and aluminium oxide nanoparticles and results indicated that the magnetic field slows the fluid flow while increasing the fluid temperature and that ethylene glycol nanofluid offers better cooling capabilities.

It has been a great challenge for the electronic and automotive industries to reduce the size needed for cooling systems while increasing their thermal performance. As a result, several researchers tried different approaches to this issue, using ethylene glycol and water in which different nanoparticles are dispersed to determine their heat transfer capabilities for automotive radiator cooling [11-16]. According to Hwang et al. [17], the thermal conductivity of the base fluid and the nanoparticles had an impact on the thermal conductivity of nanofluids. It was found that, at least for the same volume fraction, the effective thermal conductivity of the nanofluids improved with decreasing particle size. The thermal conductivity of various nanofluids like Al_2O_3-water, SiO_2-water, and TiO_2-water combinations increased by up to 30% at volume fractions of less than 4.3%. According to Peyghambarzadeh et al. [18] and Oke [19], Ethylene Glycol mixed with Al_2O_3 nanoparticles was used to enhance the cooling of vehicles. The results also demonstrated that using nanofluids in a car radiator significantly increases its cooling efficiency. The thermal conductivity of nanofluids was significantly higher than that of the base fluid water in a parametric investigation of the overall heat transfer coefficient of Copper/water in a car radiator according to [20]. The results indicated that CuO/water Nano fluids had considerably better thermal conductivity than water and that increasing the concentration of the nanofluid from 0 to 0.4 volume % results in a higher overall heat transfer coefficient. However, compared to the base fluid, the overall heat transfer coefficient increases by 8% when nanofluid is implemented at a concentration of 0.4 vol%. [21] investigated the use of ethylene glycol-based nanofluids in car radiators and found that heat transfer was enhanced in the Ethylene Glycol-based nanofluid containing CuO, Al_2O_3, and Titanium Dioxide compared to the convective fluids.

Naraki et al. [22] found that the thermal conductivity enhancement for 1 volume % Al_2O_3-water nanofluid increased from 2% at 210^oC to 10.8% at 510^oC. The improvement in thermal conductivity for 4 volume % ranged from 9.4% at 210^oC to 24.4% at 510^oC. As the bulk temperature of the nanofluid rises, the molecules and nanoparticles within it become more active as a result of increased Brownian motion, allowing for a greater rate of energy transfer between locations in a given amount of time. According to Karakas et al. [23] found that when comparing the operating temperature of a processor with that of one using a pure base fluid, the results showed that one using a blend of water and ethylene glycol produced significantly lower operating temperatures. Babu et al. [24] carried out a statistical analysis of the use of polyethylene as a reactive base fluid under the condition of thermal radiation with a moderate heat source and remarked that skin drag reduces at 47.9%. Xiu et al. [25] found that forced convection can be used to control temperature distribution in a nanofluid flow over a wedge. Ram et al. [26] reviewed several studies on base fluids and the most appropriate volume fractions for coolant.

The aforementioned literature shows base fluids like water and ethylene glycol when combined with nanoparticles, their thermal conductivity increases. It is also clear that most researchers used water as their essential base fluid, dispersed mainly with CuO and Al_2O_3 nanoparticles. The trials showed that the addition of nanoparticles improved the base fluid's thermal conductivity and this depended on several parameters which included the particle volume fraction, thermal conductivity of the base fluid, particle size, shape, and temperature. However, ethylene glycol and propylene glycol as base fluids and how their thermal properties and capabilities were affected by the addition of nanoparticles of CuO and Al_2O_3 were not extensively discussed. Further, the literature has no analysis of the relative merits of Ethylene glycol, propylene glycol, and water as a base fluid. This study works to analyze the properties of water, Propylene glycol, and ethylene glycol base fluids dispersed with CuO and MgO nanoparticles to determine the most effective base fluid nanofluid coolant for radiators. Skin friction and the Nusselt number of the underlying fluids were also studied, along with their sensitivity to the nanoparticles' presence and the magnetic field's strength.

2. Methodology

This study considers water, ethylene glycol and propylene glycol base fluids homogeneously suspended with copper oxide and magnesium oxide nanoparticles. The nanofluids of interest are water/copper oxide nanofluids, ethylene glycol/magnesium oxide, and propylene glycol/copper oxide nanofluids. The fluids under consideration are Newtonian incompressible fluids. Figure 1 describes the fluid flow pictorially. The flow is a 2D flow across a perfectly horizontal surface and it occurs in a magnetic field $\vec{B}$ whose strength is constant throughout the flow. The surface across which the fluid is flowing stretches at a constant rate of U_0 and has a temperature T_w. In the free stream, the flow is assumed to be stationary while the temperature takes the maximum temperature T_∞.

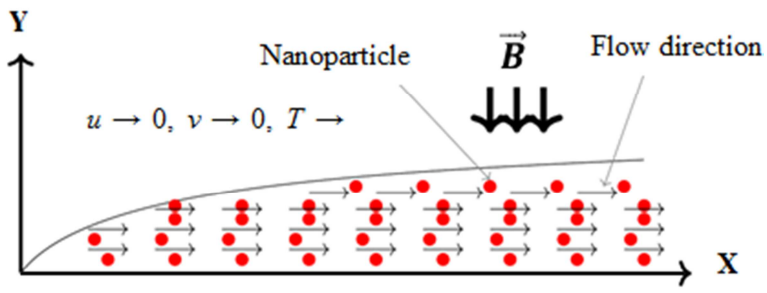

Figure 1. *Flow configuration.*

2.1. Equations for Incompressible Newtonian 2D Flow

The fluids under consideration are Newtonian and incompressible. For this reason, we assume that the density is constant in time and space and the stress tensor is proportional to the strain rate. By using the laws of conservation of mass and energy, the continuity, momentum and energy equations are derived as the Navier-Stokes equations. However, due to the complexity of the Navier-Stokes equations, the boundary layer theory is used to reduce the governing equations. In what follows, the governing equations are discussed. The continuity equation is derived from the mass conservation law for a small mass and it is generally given as

$$\frac{\partial \rho}{\partial t} + \nabla \cdot (\rho\, \vec{v}) = 0$$

Referring to the motion of a fluid that does not undergo compression, then

$$\frac{\partial \rho}{\partial t} = 0$$

and consequently, the continuity equation is $\nabla.(\rho\vec{v}) = 0 \Longrightarrow \rho\nabla.\vec{v} + \vec{v}.\nabla\rho$ and due to the incompressibility of the fluid then $\nabla\rho = 0$, hence we obtain;

$$\frac{\partial u}{\partial x} + \frac{\partial u}{\partial y} + \frac{\partial u}{\partial z} = 0.$$

The flow is 2-D then we obtain;

$$\frac{\partial u}{\partial x} + \frac{\partial u}{\partial y} = 0 \tag{1}$$

The boundary layer, the momentum and energy equations reduce to (see [27-30]),

$$u\frac{\partial u}{\partial x} + v\frac{\partial u}{\partial y} = \frac{\mu}{\rho}\frac{\partial^2 u}{\partial y^2} + g\beta(T - T_\infty) - \frac{\sigma {B_0}^2 u}{\rho}$$

$$u\frac{\partial T}{\partial x} + v\frac{\partial T}{\partial y} = \alpha\frac{\partial^2 T}{\partial y^2}$$

The no-slip condition is a stipulated condition that ensures that the fluid particles next to the surface retain the velocity of the surface and do not slide away. To ensure the no-slip boundary conditions, we have the boundary conditions stated as, $\text{at } y = 0, u = U_0, v = 0, T = T_w, \text{as } y \longrightarrow \infty;\ u = 0, T = T_\infty$

The equations governing the nanofluid are;

$$\left.\begin{gathered} \frac{\partial u}{\partial x} + \frac{\partial u}{\partial y} = 0 \\ u\frac{\partial u}{\partial x} + v\frac{\partial u}{\partial y} = \frac{\mu_{nf}}{\rho_{nf}}\frac{\partial^2 u}{\partial y^2} + g\beta_{nf}(T - T_\infty) - \frac{\sigma_{nf}{B_0}^2 u}{\rho_{nf}} \\ u\frac{\partial T}{\partial x} + v\frac{\partial T}{\partial y} = \alpha_{nf}\frac{\partial^2 T}{\partial y^2} \end{gathered}\right\} \tag{2}$$

With boundary conditions

$$\left.\begin{gathered} \text{at } y = 0, u = U_0, v = 0, T = T_w \\ \text{as } y \longrightarrow \infty;\ u = 0, T = T_\infty \end{gathered}\right\} \tag{3}$$

2.2. Solution of the Equations

Equations (2) and (3) governing the MHD flow are solved by first rescaling all the variables to lie between 0 and 1 and nondimensionalising, rewriting the equations to first-order differential equations and finally numerical procedure.

The following similarity and rescaling variables were used for the nondimensionalisation process;

$$\eta = y\left(\frac{U_0}{\vartheta_{bf}}\right)^{\frac{1}{2}}, u = U_0 x f'(\eta), v = -\left(U_0\vartheta_{bf}\right)^{\frac{1}{2}}, T = T_\infty + (T_w - T_\infty)\Theta\,(\eta)$$

The continuity equation is automatically satisfied with the choice of the similarity variables. The effective dynamic viscosity and density of the nanofluid are

$$\mu_{nf} = 0.904\mu_{bf}\, exp(0.148\phi), \rho_{nf} = (1-\phi)\rho_{bf} + \phi\rho_{np} = \left(1 - \phi + \phi\frac{\rho_{np}}{\rho_{bf}}\right)\rho_{bf}$$

and setting therefore we have

$$A_1 = \frac{\mu_{nf}}{\rho_{nf}\vartheta_{bf}} = \frac{0.904\mu_{bf}\ \exp(0.148\phi)}{\left(1-\phi+\phi\frac{\rho_{np}}{\rho_{bf}}\right)\vartheta_{bf}\rho_{bf}} = \frac{0.904\exp(0.148\phi)}{1-\phi+\phi\frac{\rho_{np}}{\rho_{bf}}}, Gr = \frac{g\beta_{nf}(T-T_\infty)}{{U_0}^2 x}, M = \frac{\sigma_{nf}{B_0}^2}{\rho_{nf}U_0}$$

The dimensionless momentum equation then becomes,

$$A_1 f''' - (f')^2 + f''f + Gr.\Theta - Mf' = 0 \tag{4}$$

Substituting the derivatives into the energy equation and using the effective thermal diffusivity, heat capacity and thermal conductivity are defined as follows;

$$\alpha_{nf} = \frac{\kappa_{nf}}{(\rho c_p)_{nf}}, \kappa_{nf} = \kappa_{bf}\left(\frac{\kappa_{np}+2\kappa_{bf}-2\phi(\kappa_{bf}-\kappa_{np})}{\kappa_{np}+2\kappa_{bf}+\phi(\kappa_{bf}-\kappa_{np})}\right) = A_2\kappa_{bf}, \left(\rho c_p\right)_{nf} = (1-\phi)\left(\rho c_p\right)_{bf} + \phi\left(\rho c_p\right)_{np} = \left(1 - \phi + \phi\frac{(\rho c_p)_{np}}{(\rho c_p)_{bf}}\right)\left(\rho c_p\right)_{bf} = A_3\left(\rho c_p\right)_{bf}\ \frac{\alpha_{nf}}{\vartheta_{nf}} = \frac{\kappa_{nf}}{(\rho c_p)_{nf}\vartheta_{nf}} = \frac{\kappa_{nf}A_2}{A_3\vartheta_{nf}(\rho c_p)_{nf}} = \frac{A_2\alpha_{bf}}{A_3\vartheta_{nf}} = \frac{A_2}{A_3 Pr}, \text{where } \frac{1}{Pr} = \frac{\alpha_{bf}}{\vartheta_{nf}}$$

The dimensionless energy equation becomes

$$\frac{A_2}{A_2}\Theta'' + Pr.\Theta' f = 0 \tag{5}$$

Considering the boundary conditions we have;

$$\left.\begin{gathered} u = U_0 x \Rightarrow U_0 x f'(0) = U_0 x, f'(0) = 1, \\ v = 0 \Rightarrow -\left(U_0\vartheta_{bf}\right)^{\frac{1}{2}} f(0) = 0, f(0) = 0 \\ T = T_w \Rightarrow T_\infty + (T_w - T_\infty)\Theta(0) = T_w \Rightarrow \Theta(0) = 1 \\ u \to 0 \Rightarrow U_0 x f'(\infty) = 0, f'(\infty) = 0, \\ T = T_w \Rightarrow T_\infty + (T_w - T_\infty)\Theta(\infty) = T_\infty \Rightarrow \Theta(\infty) = 0 \end{gathered}\right\} \tag{6}$$

Equations (4) and (5) give the dimensionless equations with

the boundary conditions;

$$f(0) = 0, f'(0) = 1, \Theta(0) = 1, f'(\infty) = 0, \Theta(\infty) = 0 \quad (7)$$

2.3. System of First Order ODEs

The equations are written in the form of first-order differential equations by setting;

$$s_1 = f, s_2 = f', s_3 = f'', s_4 = \Theta, s_5 = \Theta',$$

giving rise to the following system of equations;

$$\left.\begin{aligned} {s_1}' &= s_2 \\ {s_2}' &= s_3 \\ {s_3}' &= \frac{1}{A_1}({s_2}^2 - s_3 s_1 - Gr.s_4 + M s_2) \\ {s_4}' &= s_5 \\ {s_5}' &= -\frac{A_3 Pr}{A_2} s_5 s_1 \end{aligned}\right\} \quad (8)$$

with the conditions

$$s_1(0) = 0, s_2(0) = 1, s_4(0) = 1 \quad (9)$$

$$s_2(\infty) = 0, s_4(\infty) = 0 \quad (10)$$

where

$$Gr = \frac{g\beta_{nf}(T - T_\infty)}{{U_0}^2 x}, M = \frac{\sigma_{nf}{B_0}^2}{\rho_{nf} U_0}, A_1 = \frac{0.904\, exp(0.148\phi)}{1 - \phi + \phi\frac{\rho_{np}}{\rho_{bf}}}, A_2 = \frac{\kappa_{np} + 2\kappa_{bf} - 2\phi(\kappa_{bf} - \kappa_{np})}{\kappa_{np} + 2\kappa_{bf} + \phi(\kappa_{bf} - \kappa_{np})}, A_3 = 1 - \phi + \phi\frac{(\rho c_p)_{np}}{(\rho c_p)_{bf}}, \; Pr = \frac{\vartheta_{nf}}{\alpha_{bf}}$$

2.4. Numerical Method

The boundary conditions (10) make the problem difficult to solve using any numerical methods and therefore we use the shooting technique such that the boundary conditions (9) and (10) are written such that;

$$s_1(0) = 0, s_1(0) = 1, s_3(0) = c_1, s_4(0) = 1, s_5(0) = c_2 \quad (11)$$

The constants c_1 and c_2 are to be determined so that boundary conditions (10) are satisfied. The system of ODEs (8) will be solved with the initial conditions (11) with some guess values of c_1 andc_2. The values of c_1 and c_2 are adjusted after every solution until the boundary conditions (10) are satisfied [31]. Once the initial value problem has been established, the solution is obtained using the Runge-Kutta scheme. It is important to establish that the method of solution is accurate and this stage is called the validation stage. For the problem under consideration, we validate our results by solving the problem with both MATLAB bvp4c and MATLAB bvp5c to verify the reliability of our solution. The table below shows the output from the comparison of the two methods of solutions and a good agreement can be seen between the two results. Hence, our results are valid and reliable.

Table 1. *Validation table.*

M	Pr	Gr	C_f (bvp4c)	C_f (bvp5c)	Nu (bvp4c)	Nu (bvp5c)
3	19.61	0.1	-1.98441830604343	-1.98441832263187	3.10359097044683	3.10358512374212
3	51.83	0.1	-1.98988301735986	-1.98988310525743	5.31611416210615	5.31605018127136
3	6.9	0.1	-1.97611953235558	-1.97611953522191	1.66651502077186	1.66651457253904
3	6.9	2	-1.53969109747803	-1.53969409559968	1.74385054428305	1.74385875197664
3	6.9	4	-1.10690009814729	-1.10690017877859	1.80964865828813	1.80964829763227
3	6.9	6	-0.693528441193003	-0.693528603667917	1.86554727519571	1.86554669721541
1	6.9	0.1	-1.38903275402259	-1.38903275769784	1.79377180735402	1.79377130296389
2	6.9	0.1	-1.70750965360274	-1.70750965679532	1.72453809666098	1.72453762560866
3	6.9	0.1	-1.97611953235558	-1.97611953522191	1.66651502077186	1.66651457253904

3. Discussion of Results

This study aims at recommending a suitable nanofluid for radiator coolant therefore we explore the flow of six different nanofluids, namely; CuO-EG, MgO-EG, CuO-water, MgO-water, CuO-PG and MgO-PG nanofluids. The flow parameters are set to default values of Gr = 0.1, M = 3, and Pr = 6.9. The thermophysical properties of the six nanofluids are given in Table 2.

Table 2. *Thermophysical properties of the base fluids and the nanoparticles.*

density (ρ)		heat capacity thermal	
		(c_p) (J/kgK)	(W/mK)
Copper oxide	6510	540	18
Magnesium oxide	3580	877	42
Ethylene glycol	1114	2415	0.252
Propylene glycol	1036	2433	0.34
Pure water	997.1	4179	0.613

Figures 2 and 3 show the comparison between the three nanofluids formed by suspending CuO nanoparticles in three different base fluids. It is observed that CuO-water has the highest temperature and velocity while CuO-EG has the lowest temperature and velocity. This observation can be attributed to the thermal conductivity of CuO, the viscosity of water and the interactions at the nanoparticle-fluid interface. Copper oxide has higher thermal conductivity compared with magnesium oxide and therefore contributes to the reason CuO-water produces the highest temperature. Also, Water has the lowest viscosity among the three base fluids (water, EG and PG) and this faster flow of the nanofluid, thus the highest velocity is observed in the CuO-water. The interactions that occur at the interface between CuO nanoparticles and water base fluid are stronger due to the affinity between the water molecules and the CuO nanoparticles. Suspension of CuO nanoparticles in water creates the hydration shell around the nanoparticles which, in

turn, enhances the dispersion and prevents clogging. Meanwhile, CuO-EG and CuO-PG do not possess such affinity, making the interaction at the nanoparticle-fluid interface weaker than the one in the CuO-water nanofluid. This further explains the reason for the higher velocity of the flow.

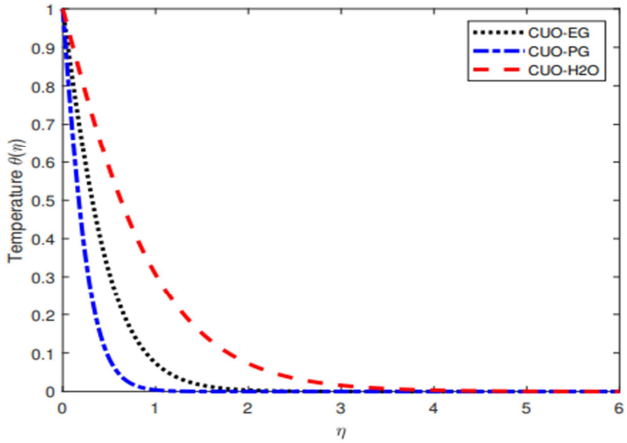

Figure 2. *Temperature comparison for CuO nanoparticles.*

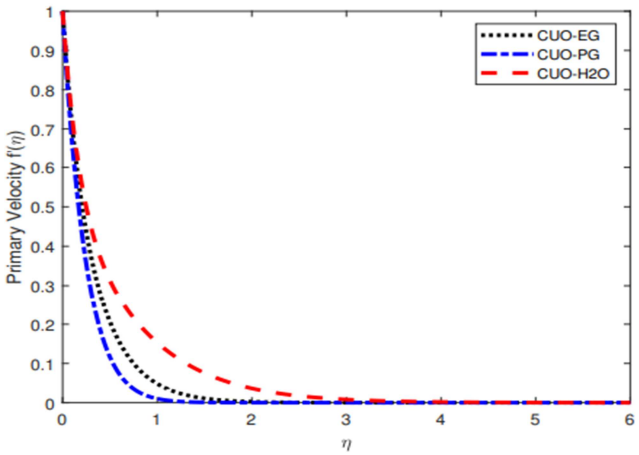

Figure 3. *Velocity comparison for CuO nanoparticles.*

The flow of the three nanofluids formed from the suspension of MgO nanoparticles in water, propylene glycol and ethylene glycol as the base fluids are compared and the results are depicted in Figures 4 and 5. The figures show that flow velocity and temperature are the highest for the MgO-water nanofluid. Dispersal of MgO in water produces a less viscous nanofluid compared to the resulting nanofluid obtained by the dispersal of MgO in ethylene glycol or propylene glycol and hence, the flow possesses a thinner viscous boundary layer. The slimmer viscous boundary layer reduces the opposition to flow, which consequently increases the flow velocity. Also, the specific heat capacity of water is higher than the other three fluids and hence, the increased temperature of flow for MgO-water.

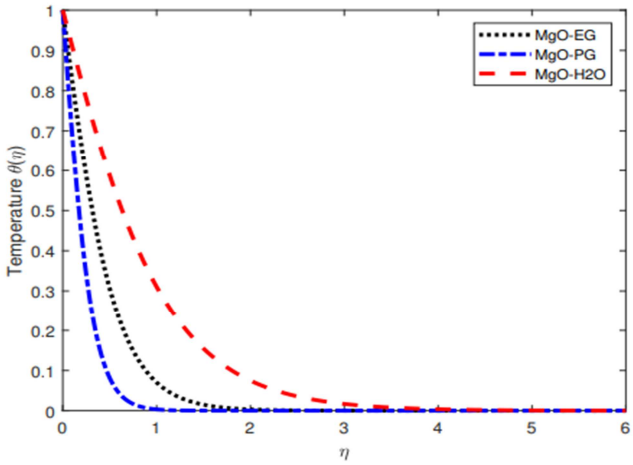

Figure 4. *Temperature comparison for MgO nanoparticles.*

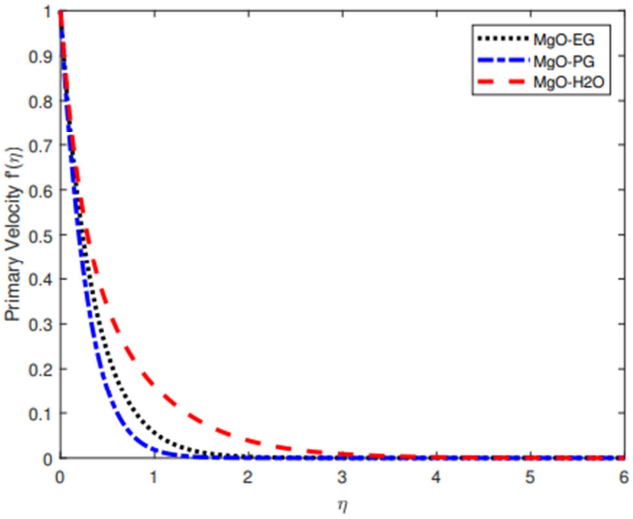

Figure 5. *Velocity comparison for MgO nanoparticles.*

The above figures show that water serves as a better base fluid for any choice of nanofluid for radiator coolant. In what follows, we investigate the influence of magnetic strength and nanoparticle volume fraction on the flow of water-based nanofluids. Figure 6 and 7 shows the behaviour of skin friction of both MgO-water and CuO-water as they flow under the influence of a magnetic field and as the volume fraction increases. As shown in Figure 6, there is the dual effect of increasing magnetic field on the skin friction. At low strength of the magnetic field, the flow is dominated by the hydrodynamic forces and since MgO has a higher affinity to water, it produces a thinner viscous boundary layer. This explains why the MgO-water nanofluid has lower skin friction when the magnetic field is not significant. As magnetic field strength becomes significant, the MgO nanoparticles are pulled out of the boundary layer towards the free stream due to their enhanced magnetism and therefore lead to an increased thickness for the viscous boundary layer. Therefore, in comparison with CuO-water nanofluid, MgO-water nanofluid possesses lower skin friction at a lower magnetic field but higher skin friction at a higher magnetic field. It is noteworthy to mention that skin

friction reduces generally with increasing magnetic field (see the downward direction of the curve in Figure 6. Figure 7 shows that increasing the volume fraction reduces skin friction.

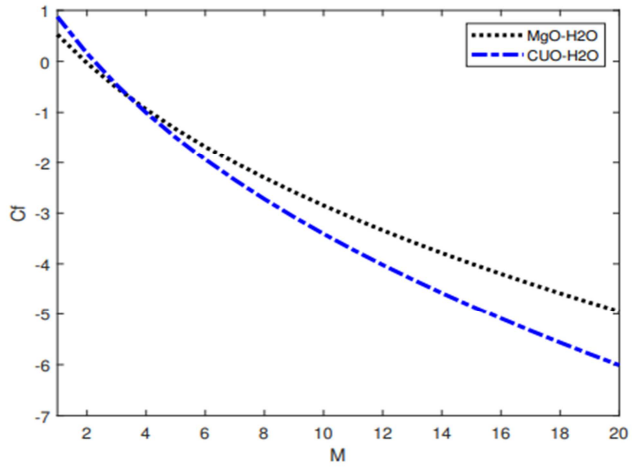

Figure 6. *Skin friction with Magnetic field for water-based nanofluids.*

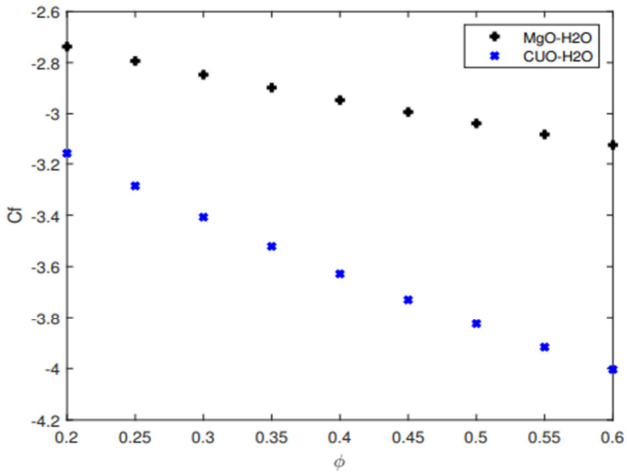

Figure 7. *Skin friction with volume fraction for water-based nanofluids.*

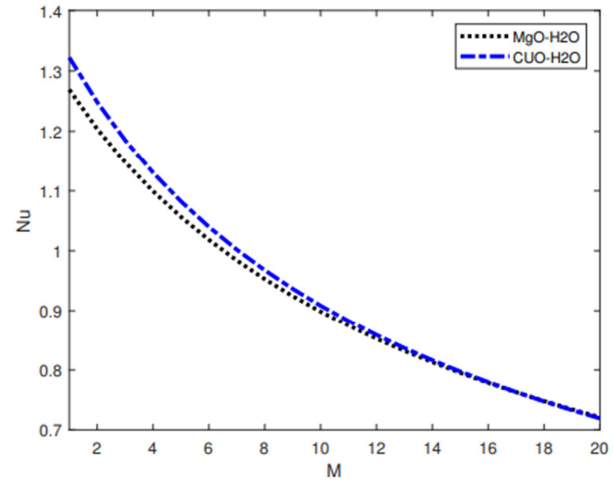

Figure 8. *Nusselt number with Magnetic field for water-based nanofluids.*

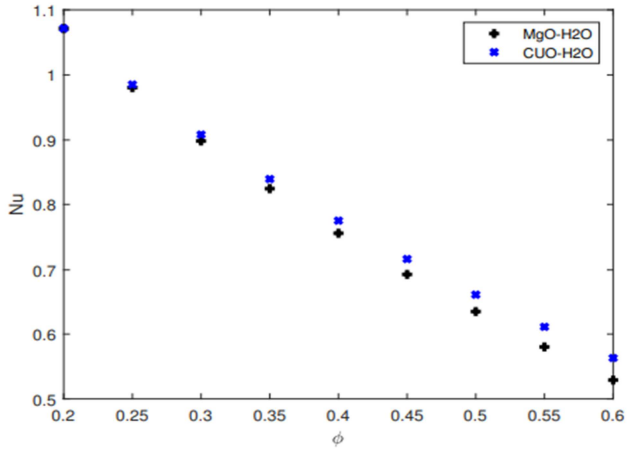

Figure 9. *Nusselt number with volume fraction for water-based nanofluids.*

The heat transfer rate reduces with increasing magnetic field as shown in Figure 8. However, it can be easily noted that CuO-water nanofluid possesses a higher heat transfer rate at a lower magnetic field. In addition, the heat transfer rate of both CuO-water and MgO-water nanofluids tend to be the same as the magnetic field increases. Therefore the use of MgO nanoparticles or CuO nanoparticles does not have any significant difference in heat transfer rate at high magnetic fields. Figure 9 shows that the heat transfer rate is not impacted by low volume fraction but by higher volume fraction. CuO-water possesses a higher heat transfer rate at a higher volume fraction.

4. Conclusion and Recommendation

4.1. Conclusion

In this study, the flows of six different nanofluids are compared. The flow is considered under the influence of magnetic and buoyancy forces and the governing equations were formulated to model the situation. Using a set of similarity variables and rescaling factors, we reduced the governing PDEs to ODEs which are later reduced to a system of first-order ODEs. The Shooting technique was used to reformulate the BVP to an IVP and the Runge-Kutta technique was used to solve the the equations. The results are validated using another method of solution and the results show good agreement. The outcomes of the study showed that;

1. water-based nanofluid has the highest flow temperature and velocity among the six nanofluids.
2. At low magnetic fields, MgO-water nanofluid has lower skin friction but CuO-water has lower skin friction at high magnetic field.
3. Increasing volume fraction reduces the skin friction for water-based nanofluids.
4. Heat transfer rate reduces with increasing magnetic field and CuO-water nanofluid possesses higher heat transfer rate at lower magnetic field.
5. At a very high magnetic field, there is no distinction in the heat transfer rate of CuO-water nanofluid and MgO-water nanofluid.

4.2. Recommendation

This study has considered the flow of three different base fluids (water, EG and PG) in which two different nanoparticles (CuO and MgO) are suspended, to determine the best nanofluid among the six possible combinations that can serve as the best radiator coolant. The study has identified that water-based nanofluids provide the best option among the three base fluids. However, depending on the closeness of the radiator to the magnetic field that emerges from the automobile engines, CuO or MgO should be considered. For instance, for a radiator located close to the magnetic field of the automobile engines, a CuO-water nanofluid is recommended while for a low magnetic field, MgO-water nanofluid is recommended.

References

[1] Choi, S. U. and Eastman, J. A. (1995). Enhancing thermal conductivity of fluids with nanoparticles.

[2] Mutuku-Njane, W. N. and Makinde, O. D. (2014). MHD nanofluid flow over a permeable vertical plate with convective heating. *Journal of Computational and Theoretical Nanoscience*, 11(3): 667–675.

[3] Oke, A. S. (2022). Combined effects of Coriolis force and nanoparticle properties on the dynamics of gold–water nanofluid across nonuniform surface. ZAMM-Journal of Applied Mathematics and Mechanics/Zeitschrift für Angewandte Mathematik und Mechanik, 102(9), e202100113.

[4] Ali, B., Ahammad, N. A., Awan, Aziz U., Oke, A. S., Tag-ElDin, E. M., Shah, F. A., Majeed, S., (2022). The dynamics of water-based nanofluid subject to the nanoparticle's radius with a significant magnetic field: The case of rotating micropolar fluid. Sustainability, MDPI, 14(17), 10474.

[5] Oke, A. S., Fatunmbi, E. O., Animasaun, I. L., Juma, B. A. (2022). Exploration of ternary-hybrid nanofluid experiencing Coriolis and Lorentz forces: case of three-dimensional flow of water conveying carbon nanotubes, graphene, and alumina nanoparticles. Waves in Random and Complex Media, Taylor & Francis, 1-20.

[6] Sekrani, G. and Poncet, S. (2018). Ethylene- and propylene-glycol based nanofluids: A litterature review on their thermophysical properties and thermal performances. *Applied Sciences*, 8(11): 2311.

[7] Areekara, S., Sabu, A. S., Mathew, A., Oke, A. S. (2023). Transport phenomena in Darcy-Forchheimer flow over a rotating disk with magnetic field and multiple slip effects: modified Buongiorno nanofluid model. Waves in Random and Complex Media, Taylor & Francis, 43831, 1-20.

[8] Ali, B., Ahammad, N. A., Windarto; Oke, A. S., Shah, N. A., Chung, J. D. (2023). Significance of Tiny Particles of Dust and TiO2 Subject to Lorentz Force: The Case of Non-Newtonian Dusty Rotating Fluid. Mathematics, MDPI, 11(4), 877.

[9] Murshed, S., Leong, K., and Yang, C. (2009). A combined model for the effective thermal conductivity of nanofluids. *Applied Thermal Engineering*, 29(11-12): 2477–2483.

[10] Kimulu, A. M., Mutuku, W. N., and Mutua, N. M. (2018). Car Antifreeze and Coolant: Comparing Water and Ethylene Glycol as Nano Fluid Base Fluid. *International Journal of Advances in Scientific Research and Engineering*, 4(6): 17–37.

[11] Aglawe, K. R., Yadav, R. K., and Thool, S. B. (2021). Preparation, applications and challenges of nanofluids in electronic cooling: A systematic review. *Materials Today: Proceedings*, 43: 366–372. 1st International Conference on Energy, Material Sciences and Mechanical Engineering.

[12] Venugopal, T., Pendli, S., Patel, H., Gupta, M., and Natarajan, G. (2022). The Performance of an Automobile Radiator with Aluminum Oxide Nanofluid as a Coolant—An Experimental Investigation. In *SAE Technical Paper Series*. SAE International.

[13] Su, C.-Q., Wang, S., Liu, X., Tao, Q., and Wang, Y.-P. (2022). Experimental and numerical investigation on spray cooling of radiator in fuel cell vehicle. *Energy Reports*, 8: 1283–1294. 2021 The 8th International Conference on Power and Energy Systems Engineering.

[14] Animasaun, I. L., Oke, A. S., Al-Mdallal, Q. M., Zidan, A. M. (2023). Exploration of water conveying carbon nanotubes, graphene, and copper nanoparticles on impermeable stagnant and moveable walls experiencing variable temperature: thermal analysis. Journal of Thermal Analysis and CalorimetrySpringer International Publishing, 148(10), 4513-4522.

[15] Oke, A. S., Eyinla, T., Juma, B. A., (2023). Effect of Coriolis Force on Modified Eyring Powell Fluid flow. Journal of Engineering Research and Reports, 24(4), 26-34.

[16] Rani, K. S., Reddy, G. V. R., Oke, A. S. (2023). Significance of Cattaneo-Christov Heat Flux on Chemically Reacting Nanofluids Flow Past a Stretching Sheet with Joule Heating Effect. CFD Letters, 15(7), 31-41.

[17] Hwang, Y., Lee, J., Lee, C., Jung, Y., Cheong, S., Lee, C., Ku, B., and Jang, S. (2007). Stability and thermal conductivity characteristics of nanofluids. *Thermochimica Acta*, 455(1-2): 70–74.

[18] Peyghambarzadeh, S., Hashemabadi, S., Jamnani, M. S., and Hoseini, S. (2011). Improving the cooling performance of automobile radiator with al2o3/water nanofluid. *Applied Thermal Engineering*, 31(10): 1833–1838.

[19] Oke, A. S. (2022). Heat and mass transfer in 3D MHD flow of EG-based ternary hybrid nanofluid over a rotating surface. Arabian Journal for Science and Engineering, Springer Berlin Heidelberg Berlin/Heidelberg, 47(12), 16015-16031.

[20] Naraki, M., Peyghambarzadeh, S., Hashemabadi, S., and Vermahmoudi, Y. (2013). Parametric study of overall heat transfer coefficient of CuO/water nanofluids in a car radiator. *International Journal of Thermal Sciences*, 66: 82–90.

[21] Mutuku, W. N. (2016). Ethylene glycol (EG)-based nanofluids as a coolant for automotive radiator. *Asia Pacific Journal on Computational Engineering*, 3(1).

[22] Soylu, S. K., Atmaca, I., Asiltürk, M., and Dogan, A. (2019). Improving heat transfer performance of an automobile radiator using Cu and Ag doped TiO2 based nanofluids. *Applied Thermal Engineering*, 157: 113743.

[23] Karakas, A., Harikrishnan, S., and Oztop, H. F. (2022). Preparation of EG/water mixture-based nanofluids using metal-oxide nanocomposite and measurement of their thermophysical properties. *Thermal Science and Engineering Progress*, 36: 101538.

[24] Babu, M. J., Rao, Y. S., Kumar, A. S., Raju, C., Shehzad, S., Ambreen, T., and Shah, N. A. (2022). Squeezed flow of polyethylene glycol and water based hybrid nanofluid over a magnetized sensor surface: A statistical approach. *International Communications in Heat and Mass Transfer*, 135: 106136.

[25] Xiu, W., Animasaun, I. L., Al-Mdallal, Q. M., Alzahrani, A. K., and Muhammad, T. (2022). Dynamics of ternary-hybrid nanofluids due to dual stretching on wedge surfaces when volume of nanoparticles is small and large: forced convection of water at different temperatures. *International Communications in Heat and Mass Transfer*, 137: 106241.

[26] Ram, S., Yadav, S. K., and Kumar, A. (2023). Recent advancement of nanofluids in solar concentrating collectors: A brief review. *Materials Today: Proceedings*, 72: 2032–2038.

[27] Oke, A. S., (2021). Coriolis effects on MHD flow of MEP fluid over a non-uniform surface in the presence of thermal radiation. International Communications in Heat and Mass Transfer, Pergamon, 129, 105695.

[28] Oke, A. S., (2022). Theoretical analysis of modified Eyring Powell fluid flow. Journal of the Taiwan Institute of Chemical Engineers, Elsevier, 132, 104152.

[29] Oke, A. S., Prasannakumara, B. C., Mutuku, W. N., Gowda, R. J. P., Juma, B. A., Kumar, R. N., Bada, O. I. (2022). Exploration of the effects of Coriolis force and thermal radiation on water-based hybrid nanofluid flow over an exponentially stretching plate. Scientific Reports, Nature Publishing Group UK London, 12(1), 21733.

[30] Juma, B. A., Oke, A. S., Ariwayo, A. G., Ouru, O. J. (2022). Theoretical Analysis of MHD Williamson Flow Across a Rotating Inclined Surface. Applied Mathematics and Computational Intelligence, 11(1), 133 – 145.

[31] Oke, A. S. (2017). Convergence of Differential Transform Method for Ordinary Differential Equations. Journal of Advances in Mathematics and Computer Science, 6, 42736.